

1 ***Recyclable-by-design mono-material flexible packaging with high barrier properties realized***
2 ***through graphene hybrid coatings***

3

4 Marco Guerriatore^a, Federico Olivieri^a, Rachele Castaldo^{a,*}, Roberto Avolio^a, Mariacristina Cocca^a,
5 Maria Emanuela Errico^a, Maria Rosaria Galdi^b, Cosimo Carfagna^{a,c}, Gennaro Gentile^a

6

7 a) Institute for Polymers Composites and Biomaterials – National Research Council of Italy (IPCB-CNR), Via Campi Flegrei
8 34, 80078 Pozzuoli (NA), Italy

9 b) Flex Packaging AL SpA, Via G. Vitale, 84013 Cava de Tirreni (SA), Italy

10 c) CRdC Nuove Tecnologie per le Attività Produttive Scarl, Via Nuova Agnano 11, 80125 Naples, Italy

11

12 * Corresponding Author: Rachele Castaldo, rachele.castaldo@cnr.it

13

14 **Highlights**

- 15
- 16 • A design-for-recycling approach has been applied to realize high performance films for packaging applications.
 - 17 • Mono-material polyolefin flexible films with remarkable barrier properties to gases and UV radiation have been developed by applying coatings based on graphene derivatives.
 - 18 • The applied coatings show very regular morphology, and do not alter the flexibility and the overall mechanical properties of the substrates.
 - 19 • The applied coatings show very regular morphology, and do not alter the flexibility and the overall mechanical properties of the substrates.
 - 20 • The applied coatings show very regular morphology, and do not alter the flexibility and the overall mechanical properties of the substrates.
 - 21 • The new barrier films are easy recyclable, as demonstrated by their reprocessing by extrusion and compression moulding.
 - 22 • The new barrier films are easy recyclable, as demonstrated by their reprocessing by extrusion and compression moulding.
 - 23 • The proposed materials represent a promising solution to realize polymer based high performance mono-material products with a sustainable end-of-life option.
 - 24 • The proposed materials represent a promising solution to realize polymer based high performance mono-material products with a sustainable end-of-life option.

25

26 **Abstract**

27 Due to the large production of plastic packaging, packaging mismanagement represents a significant
28 problem for the environment and the related economic/social contexts. A new route towards
29 sustainable recycling has been identified in the design of the plastic products together with their
30 end-of-life recycling options. Following this approach, in this work, new recyclable-by-design mono-
31 material flexible films with high barrier properties to gases and UV radiation have been developed
32 by applying graphene oxide (GO) and graphene oxide/montmorillonite (GO/MMT) hybrid coatings
33 on polyolefin substrates. The coatings induce a remarkable reduction of the UV transmittance (40-

34 60%) and of the oxygen (94-99%) and water vapour (68-73%) permeability of the films, with very
35 good stability after prolonged water immersion. Reprocessing tests demonstrate the easy
36 recyclability of the coated films, whose commercial analogues are currently considered as non-
37 recyclable. By extrusion and compression moulding, recycled films are obtained in which the
38 nanostructured phases result well embedded in the polymer matrices. The mechanical properties
39 of the samples obtained by reprocessing coated polyethylene and polypropylene films are
40 comparable to those of the reprocessed pristine films. Moreover, no significant release of GO by
41 water immersion for 24h at room temperature is detected from the recycled samples. Overall, the
42 results indicate that the application of thin GO/MMT coatings to realize mono-material barrier films
43 for packaging applications is an effective strategy to realize high performance products able to be
44 easily recycled. These mono-material flexible films represent a new sustainable end-of-life option
45 with respect to current commercial multi-layer products.

46

47 **1. Introduction**

48 Protection, aimed at increasing the useful life of the products, is a fundamental objective in the
49 packaging sector. This concept is even more important in the case of the food packaging industry,
50 with the scope of delaying the deterioration of food and guaranteeing high quality and safety by
51 providing chemical, physical and biological protection (Marsh & Bugusu, 2007). In this perspective,
52 plastic food packaging should contribute to promote an increased circularity in the food supply
53 chain, replying to the key challenge of saving food and resources (Despoudi, 2020). Thus, the
54 development of a new generation of sustainable food packaging should be able to reduce food
55 losses and face safety issues, by preventing food-borne diseases and contamination, being at the
56 same time reusable/recyclable, thus contributing to an overall preservation of the environment
57 (Guillard et al., 2018).

58 Oxygen and light are the main causes of most food degradation processes. Oxygen promotes the
59 oxidation of fats, the loss of nutrients and vitamins and the growth of aerobic microorganisms (Liu
60 et al., 2010). UV light can affect food quality generating free radicals by a number of organic
61 photochemical reactions. Moreover, UV irradiation can induce an early decrease of the food quality,
62 altering food flavour and colour, promoting the degradation of vitamins, proteins and food
63 antioxidants, and generating toxic substances (Goudarzi et al., 2017).

64 For these reasons, the food packaging industry has always attempted to develop and exploit ever
65 more effective materials acting as barrier to gases and light. Most of the currently available
66 commercial barrier packaging solutions include multilayer flexible films having complex structures.
67 These films are generally constituted by plastics and aluminium layers, by different plastic layers
68 and/or by different plastics and metallized plastic layers. When different materials are combined in
69 a single product by lamination or by co-extrusion, the technical advantages obtained in terms of
70 better performances are paid for in terms of their recyclability. In fact, multi-component multi-
71 layered packaging cannot be recycled using traditional plastic reprocessing technologies, such as
72 mechanical recycling, due to the chemical incompatibility of the different layers (Barlow & Morgan,
73 2013; Ma, 2018). One of the most investigated solutions to recycle multi-component multi-layered
74 packaging materials is based on their delamination in order to separate the different components
75 and to recycle them separately (Anukiruthika et al., 2020). Other approaches are based on the
76 selective dissolution of one polymer phase (Walker et al., 2020) or on the simultaneous processing
77 of immiscible polymer phases and eventually the aluminium phase, in presence of suitable
78 compatibilizing or process aid agents (Avella et al., 2009; Kaiser et al., 2018; Yang et al., 2018).

79 Nevertheless, the proposed solutions are still not technically or economically sustainable, and
80 therefore multi-material flexible packaging films are currently landfilled or used for energy recovery
81 (Horodytska et al., 2018; Mourad et al., 2008).

82 **The design-for-recycling approach for flexible packaging films.** An effective approach to promote
83 higher recycling rates of plastic products, at the basis of current industrial objectives and trends, is
84 the design-for-recycling approach,

85 In this context, the packaging industry has already identified high performance mono-material
86 plastic packaging, constituted by a single polymer and without any continuous metal layer, an
87 effective step towards the goal of recyclable-by-design products that could: i) significantly reduce
88 the complexity of packaging products; ii) decrease the amount of non-recyclable fractions, including
89 barrier agents and inks towards mono-materials, with preference for mono-PE and mono-PP; iii)
90 reduce the fluctuation of the quality and quantity of recycled products delivered to consumers; iv)
91 avoid the wrong social perception that recycled plastics could have inferior quality or even being
92 unsafe for human health (Ahamed et al., 2021; Eriksen et al., 2019; Grace, 2019; Pettersen et al.,
93 2020, RecyClass, Recyclability Methodology, 2020; Plastics Recyclers Europe, Challenges and
94 Opportunities, 2021; Ceflex, Designing for a Circular Economy, An Introduction, 2020).

95 In particular, polyolefin mono-material flexible films have been reported as interesting products
96 able to meet the requirements of circular economy because of their easy mechanical recyclability
97 (Barlow & Morgan, 2013; Ragaert et al., 2020; Srebrenkoska et al., 2009). Due to the low amount of
98 additives, polymer nanocomposites represent a typical example of mono-material. Since 1985, the
99 year of the Toyota polyamide/montmorillonite nanocomposite (Okada & Usuki, 2006), plenty of
100 researches aimed at realizing gas barrier nanocomposite films by effectively dispersing functional
101 nanofillers with different aspect ratio in bulky polymer matrices (Gusev & Lusti, 2001). In these
102 works, the tortuous path mechanism (Ellis & D'Angelo, 2003) and the interfacial effect (Avella et al.,
103 2007; Avolio et al., 2013; Scherillo et al., 2014) have been exploited, both able to reduce the rate of
104 gas diffusion through the material. Nevertheless, despite the high expectation, until now these
105 types of nanocomposites with improved gas barrier properties have largely failed to reach the
106 market for food packaging applications. More recently, approximately since 2005, a change of
107 paradigm occurred, and the research moved towards the development of nanostructured gas
108 barrier coatings on flexible mono-polymer films (Rovera et al., 2020). In the years, this approach has
109 been considered ever more promising and effective for the industry because the nanostructures
110 applied in coatings, rather than being randomly dispersed in the polymer matrix, are confined to

111 the external surface of the polymer films, and thus they do not modify the thermomechanical
112 properties and the processability of the polymer substrate.

113 Due to their high aspect ratio and their ability to maximize the effect of the tortuous path
114 mechanism, different 2D materials have been tested for high barrier coating applications (Yu et al.,
115 2021). Montmorillonite and related nanocomposites (Chen et al., 2015; Findenig et al., 2012; Lim et
116 al., 2021) have been widely investigate to realize coatings with reduced gas permeability on
117 different flexible films. Layered double hydroxide (LDH) nanosheets dispersions were recently
118 applied onto polyethylene terephthalate (PET) to realize high performance coatings with very low
119 permeability towards oxygen and water vapour and described as able to replace metallized multi-
120 layered packaging products (Ruengkajorn et al., 2021; Yu et al., 2019). Graphene derivatives were
121 also considered as potential highly effective barrier agents on various flexible polymer substrates
122 (Pierleoni et al., 2016; Won et al., 2018). Investigating on graphene coatings, researchers were able
123 to understand how tailoring the self-assembled structures can enhance the gas barrier properties
124 of the systems (Castaldo et al., 2018; Scherillo et al., 2014; Yan et al., 2015). Hybrid nanostructures
125 constituted by graphene derivatives and phyllosilicates were also the subject of interesting
126 researches, demonstrating their enhanced gas barrier properties when graphene sheets self-
127 assembled with the platelets of the phyllosilicate component in well oriented nanostructures
128 (Castaldo et al., 2019; Yoo et al., 2014). Nevertheless, only a few papers report on the
129 recycling/reprocessing of polyethylene (Asmatulu et al., 2015), polypropylene (Triantou et al., 2017)
130 and other polymers or polymer blends containing nanoparticles (Botta et al., 2018; Pang et al.,
131 2021). Moreover, some papers report remarkable results on the recycling of polymer/clay
132 nanocomposites (Chowreddy et al., 2019; Rigail-Cedeño et al., 2019).

133 **Layout and impact of the study.** In summary, the large use of multilayer films in plastic packaging
134 represents a barrier that strongly reduces the sustainable recycling options for these materials at
135 the end of life. The impact of this problem is well represented by the EU production of plastic
136 packaging, that exceeded 20 million tonnes in 2020 (PlasticsEurope, Plastics – the Fact 2020 report,
137 2020). It is estimated that only 5% of the value of the plastic packaging material remains within the
138 economic cycle and that 95% is lost after the first use, which usually turns out to be very short since,
139 even today, despite the efforts of institutions and consumers, most plastics are not recycled
140 (European Commission, Questions & Answers: A European strategy for plastics, 2018). This also
141 happens due to how the products are designed and due to the presence of non-recyclable or multi-
142 layered materials. The main properties required for the successful adoption of mono-material films

143 in the packaging sector have been identified as: suitable mechanical strength and gas/vapour
144 barrier; low material and processing cost; efficient recyclability with conventional processing
145 technologies at the end of life.

146 This work aim to address all of this points, by demonstrating the effectiveness and recyclability-by-
147 design of mono-material films. Polyolefins were selected as the most used polymers for packaging
148 materials, and their barrier properties were improved by the application of nanostructured GO and
149 GO/clay hybrid coatings, deposited by a simple and scalable system. After the assessment of physical
150 properties, the recyclability of the films was demonstrated by reprocessing them and testing the
151 recycled materials.

152

153 **2. Experimental section**

154 *2.1 Materials*

155 Polyethylene and polypropylene cast films were supplied by Flex Packaging AL S.p.A. (Cava de'
156 Tirreni, Italy). In particular, a 70 μm thick LDPE film (density of 0,924 g/cm^3 , ASTM-D792) and a 50
157 μm thick PP film (density of 0,9 g/cm^3 , ASTM D 1505), both corona treated, with a surface tension >
158 38 dyne/cm were used. These samples were coded PE and PP, respectively.

159 Graphene oxide (GO) water dispersion (4.5 g/L) was purchased from Nanesa S.r.l. (Arezzo, Italy),
160 cloisite Na^+ (MMT) was purchased from BYK Additives & Instruments (Wesel, Germany). All the
161 other solvents and reagents were obtained from Merck KGaA (Darmstadt, Germany) and used
162 without further purification.

163

164 *2.2 Application of GO and GO-MMT coatings onto flexible films*

165 The application of the GO coating onto PE and PP films was carried out using a rod coater "K hand
166 coater" (Royston, United Kingdom). The GO dispersion was diluted with distilled water until a
167 concentration of 3.1 g/L. The treatment on the PE and the PP films was performed applying an
168 amount of water dispersion tailored to obtain coatings whose dry weight was approximately 280
169 mg/m^2 . The corresponding thickness of the coatings was in the approximate range 140-200 nm,
170 corresponding to volume fractions of 0.2-0.3 vol% for the PE based systems and 0.3-0.4 vol% for the
171 PP based systems. The obtained samples were named PE-GO and PP-GO.

172 For the preparation of GO-MMT hybrid coatings, MMT was dispersed in distilled water at 3.1 mg/mL
173 concentration by sonication with a Sonics Vibracell ultrasonic processor (Newton, USA) (500 W, 20
174 kHz), at 25% of amplitude for 30 min, with 30 s/30 s on/off cycles. Then, the dispersion was mixed

175 in equicomposition with GO and the resulting dispersion was sonicated at the same conditions for
176 10 minutes. Finally, 280 mg/m² GO-MMT hybrid coatings were obtained on PE and PP using a rod
177 coater obtaining, also in this case, coatings of 140-200 nm approximate thickness. These samples
178 were coded PE-GO-MMT and PP-GO-MMT and were characterized by the same coating volume
179 fraction of PE-GO and PP-GO.

180

181 *2.3 Recycling*

182 Before processing, differential scanning calorimetry (DSC) and melt flow rate (MFR) analyses were
183 performed on PE and PP pristine films.

184 DSC measurements were performed by means of a TA-Q2000 differential scanning calorimeter
185 equipped with a RCS-90 cooling unit (TA Instruments). The instrument was calibrated in
186 temperature and energy with pure indium. The samples were sealed into a Tzero aluminum pan.
187 Measurements were performed from 25 °C to 250 °C at 10 °C/min heating rate. High-purity nitrogen
188 gas was fluxed at 20 mL/min during the measurements.

189 MFR analyses were performed by means of an Instron CEAST MF20 following the ASTM D1238 test
190 conditions, at 190 °C and using a weight of 2.16 kg.

191 Reprocessing tests were carried out on flexible films based on PE and PP treated with GO and GO-
192 MMT barrier coatings (PE-GO, PP-GO, PE-GO-MMT, PP-GO-MMT). The films were extruded using a
193 Thermo Scientific HAAKE MiniLab II Rheology Solutions twin screw micro compounder. The
194 processing time was set at 10 minutes in order to allow a sufficient melt mixing. The PE-based films
195 were extruded at 135 °C with screw speeds of 30 rpm. The PP-based films were extruded at 165 °C
196 with screw speeds of 30 rpm until the films were completely inserted, subsequently the speed was
197 increased to 60 rpm. After cooling and pelletization, films about 100 µm thick were obtained by
198 compression moulding using a hot platen press Dr Collin K40. The plates temperature was set at 140
199 °C for the PE-based systems and at 180 °C for the PP-based systems. The moulding time was fixed
200 at 6 min and the pressure at 100 bar. After this cycle, the samples were quickly cooled by rapid
201 insertion of the cooling cassette system. The so obtained recycled samples were coded with the
202 same codes used for the starting materials, only adding the suffix _R: PE-GO_R, PE-GO-MMT_R, PP-
203 GO_R, PP-GO-MMT_R. The neat PE and PP films, without coatings, were processed under the same
204 conditions for comparison, obtaining the recycled films PE_R and PP_R.

205

206 *2.4 Characterization*

207 UV-visible spectra were recorded for all the samples by means of a Jasco V570 UV
208 spectrophotometer in the range 200-800 nm.

209 Scanning electron microscopy (SEM) analysis was performed on the surface of PE-GO, PP_GO, PE-
210 GO-MMT and PP-GO-MMT and on the cryogenically fractured cross sections of the recycled
211 samples. The analyses were performed with a FEI Quanta 200 FEG SEM using a secondary electron
212 detector and an acceleration voltage of 10–30 kV. Before the analysis the samples were sputter
213 coated with gold/palladium.

214 Transmission electron microscopy (TEM) analysis was performed on the recycled samples. Ultrathin
215 sections (nominal thickness 100 nm) of the specimens were realized with a Leica EM FC6-UC6 cryo-
216 ultramicrotome system operating at -100 °C for PE-GO_R and PE-GO-MMT_R and at room
217 temperature for PP-GO_R and PP-GO-MMT_R. The sections were then placed on 400 mesh copper
218 grids and observed in bright field mode on a FEI Tecnai G12 Spirit Twin TEM operating at 120 kV
219 acceleration voltage.

220 Oxygen transmission rate measurements were performed on all samples using a Multiperm
221 Extrasolution Permeabilimeter at 25 °C and 10 % RH.

222 Water vapor transmission rate was measured for all the samples using the cup method (ASTM E96)
223 at 25 °C using a difference in RH of 50 % between the inside (RH 100 %) and the outside (RH 50 %)
224 of the testing cup.

225 The stability of the coatings in water was evaluated through a test designed in order to evaluate the
226 eventual migration of the nanostructured coating in water based lacquers, paints or inks, using
227 distilled water as simulant. Samples with a diameter of 40 mm were placed in a sealed Petri dish
228 containing 8 mL of distilled water and stored for 24 h at 25°C. The amount of graphene oxide
229 migrating to water was measured by analysing the aqueous media by UV-visible spectroscopy.
230 Further details on this procedure are reported in Supplementary Information and the GO calibration
231 curve in water is reported in Figure S1. The same method was applied to evaluate the release of GO
232 from the recycled films.

233 A FTA 1000 (First Ten Ångstroms) instrument was used to measure static contact angles (CA) of
234 pristine PE and PP films and the coated films. The samples were attached on a double-sided tape
235 applied on a microscope glass slide and a 7.5 µL distilled water droplet was positioned on the film
236 surface. Each measurement was repeated on six different areas of the sample. The experiments
237 were conducted at room temperature. CA was geometrically evaluated as the angle formed by the
238 solid surface and the tangent to the droplet. Reported data are the average of the measured values.

239 The recycled films were characterized by tensile tests using an Instron 5564 with a strain rate of 10
240 mm/min. Dumbbell samples were used with an average thickness of 100 μm , and a gauge length of
241 20 mm. Young's modulus, yield stress and elongation at break were obtained by statistical analysis
242 of the results obtained on 10 tested specimens for each sample, calculating the average and the
243 standard deviation values. PE and PP pristine films were tested in the same conditions for
244 comparison.

245 The pristine PP film and the recycled PP_R film were analyzed by Fourier transform infrared (FTIR)
246 spectroscopy in attenuated total reflectance (ATR) mode using a PerkinElmer Spectrum One FTIR
247 spectrometer equipped with an ATR module, using a resolution of 4 cm^{-1} and 32 scan collections.
248 Also, PP_R was analysed by DSC using the above mentioned equipment, in order to evaluate PP and
249 PP_R crystallinity degrees.

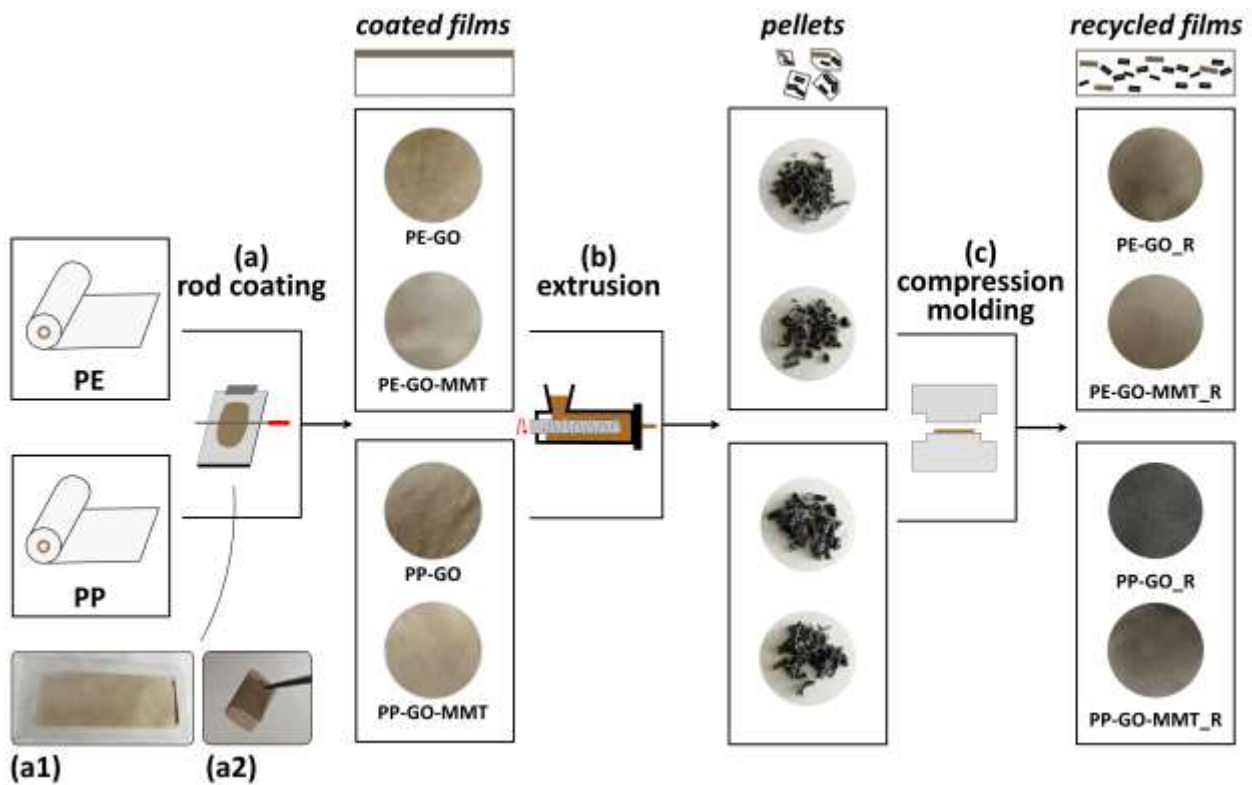
250

251 **3. Results and discussion**

252 *3.1 Barrier coatings*

253 The overall scheme of the work performed, with the images of the obtained samples, is reported in
254 Figure 1. After application of the GO and GO/MMT hybrid coatings by rod coater, coated samples
255 of PE and PP films wide about 10 cm and long about 30 cm were obtained, shown in Figure 1(a1).
256 For both the substrates, the films remained highly flexible, as illustrated in Figure 1(a2). The coated
257 PE and PP films exhibited a light brown colour, which for both the substrates was more intense for
258 the GO-coated samples and slightly less intense for the GO-MMT-coated samples, as shown in
259 Figure 1, left column (coated films).

260



261

262 Figure 1. Overall scheme of the work, evidencing the three phases: a) coating application, with the images
 263 of the obtained samples, and with details showing the coated films realized by rod coating (a1) and the
 264 flexibility of the coated films (a2); b) reprocessing of the coated substrates by extrusion, with the images of
 265 the obtained reprocessed pellets; c) compression moulding of the reprocessed films, with the images of the
 266 obtained recycled films
 267

268 UV-visible spectra (Figure S2) were collected on the pristine and coated samples in order to evaluate
 269 the reduction in transmittance caused by the coating application. All coated films show lower
 270 transmittance than the pristine PE or PP substrates in all the investigated range (200-800 nm), with
 271 a steep decrease of the transmittance at lower wavelength. Transmittance at 400 nm and
 272 transmittance reduction with respect to the corresponding uncoated substrate are reported in Table
 273 1. As shown, GO coatings showed a transmittance reduction at 400 nm of about 60% with respect
 274 to the pristine films. In agreement to the visual analysis, the GO-MMT coatings showed a lower
 275 transmittance reduction, ranging between 41.4% (for PE-GO-MMT) and 48.1% (for PP-GO-MMT).
 276

277 Table 1. Transmittance and transmittance reduction at 400 nm, oxygen and water vapour transmission rate
 278 (OTR and WVTR) of pristine and coated PE and PP films
 279

Sample	Transmittance (%) at 400 nm	Transmittance reduction (%) at 400 nm ^a	OTR [cm ³ *mm/(24h*m ²)]	WVTR [g*mm/(24h*m ²)]
PE	75.3	-	246	0.195

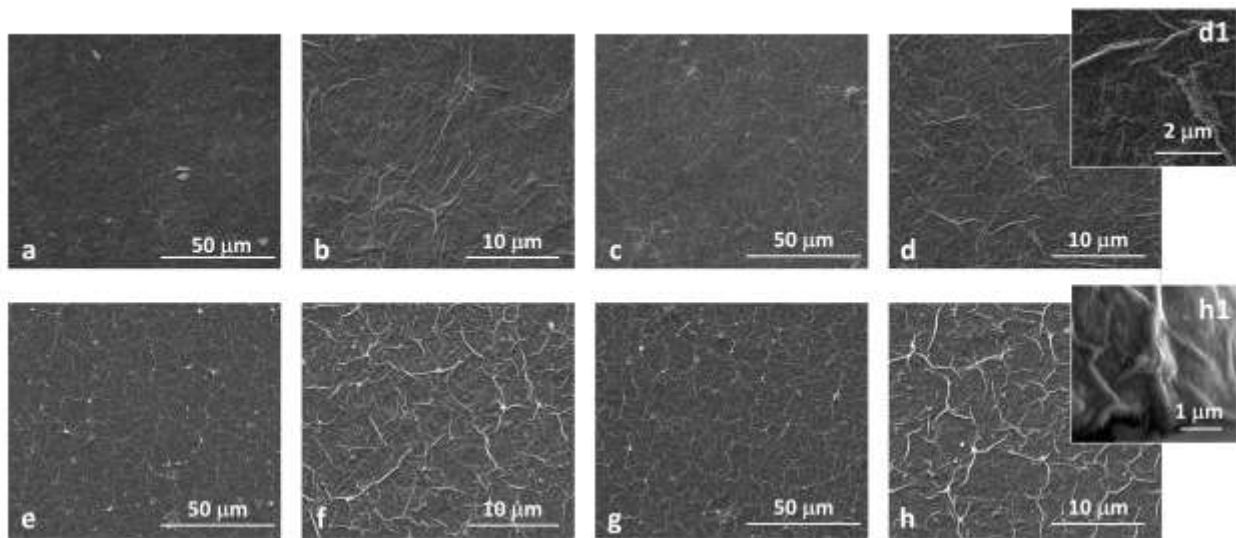
PE-GO	17.1	58.2	6	0.053
PE-GO-MMT	34.0	41.4	4	0.061
PP	80.0	-	93	0.166
PP-GO	19.9	60.1	3	0.035
PP-GO-MMT	31.9	48.1	6	0.049

280 ^a standard deviation values < 2%

281

282 The morphology of the applied coatings was investigated by SEM analysis. SEM images of the coated
 283 films show that all the samples are highly homogeneous, with wrinkles due to the coalescence and
 284 subsequent deformation of the GO and MMT flakes during the water evaporation process, see
 285 Figure 2. GO-MMT coatings showed more pronounced wrinkles, indicating that the interactions
 286 between the graphene sheets and the phyllosilicate lamellae gave rise to hybrid morphologies. In
 287 addition, in the PE-GO-MMT and PP-GO-MMT samples sporadic particles smaller than 500 nm were
 288 evidenced on the film surface, due to the presence of poorly-dispersible clay residues in the water
 289 formulation applied on the film surface.

290



291

292 Figure 2. SEM images of PE-GO (a, b), PP-GO (c, d), PE-GO-MMT (e, f) and PP-GO-MMT (g, h)

293

294 Oxygen and water vapour permeability tests were performed on the PE and PP samples coated with
 295 either GO and GO-MMT layers. Results are summarized in Table 1. As shown, the effect of the
 296 coating on the gas barrier properties was very pronounced for both the investigated systems. For
 297 what concerns the polyethylene substrate, coatings induced a reduction of the OTR of about 97.5%
 298 for GO and about 98.5% for GO-MMT, and a WVTR reduction of about 72.5% for GO and 68.0% for
 299 the hybrid GO-MMT. Similarly, for the PP substrate, the decreases of the OTR were 96.5% and 94.0%

300 for GO and the GO-MMT hybrid coating, respectively, while the WVTR decreases were found
301 respectively 78.8% and 70.4%.

302 The final OTR and WVTR values were comparable or even better than the values reported in
303 literature for different classes of coatings. In particular, the developed systems showed comparable
304 or better performances than:

305 - spray-assisted layer-by-layer (LbL) GO based coatings applied on polyethylene, which induced a
306 reduction of 69 % of the OTR (Heo et al., 2019), and LbL polyvinyl alcohol (PVOH)/rGO coatings
307 applied on PET, which induced a 92 % reduction of OTR and a 30 % reduction of WVTR of the
308 substrate (Zhan et al., 2021);

309 - SiO_x coatings on PE that showed a reduction of about 90% of the OTR (Li et al., n.d.), and SiO_x
310 coatings on PP, that showed a 95.5 % OTR decrease and a reduction of about 80.3 % of the WVTR
311 (Kirchheim et al., n.d.);

312 - AlO_x coatings on PP, that showed about 90 % decrease of the OTR (Hirvikorpi et al., 2010) and
313 WVTR (Struller et al., 2014);

314 - polyvinylidene chloride (PVDC) coatings applied on PET, that showed 95 % OTR reduction with
315 respect to the pristine polymer (Rovera et al., 2020),

316 Comparing the coating propose in this work with the above listed systems, it is to be taken into
317 account that these SiO_x and AlO_x ceramic coatings are obtained by chemical vapour deposition
318 techniques, such as dielectric barrier discharge (DBD) plasma or atomic layer deposition (ALD),
319 which are far more complex and expensive than coatings applied by rod coating deposition.
320 Moreover, concerning PVDC, one should consider that the use of chlorinated products is being
321 gradually restricted from many packaging applications, since they are still under investigation for
322 their difficult and possible unsafe recyclability, because during high temperature reprocessing they
323 can leach out harmful chemicals for the environment and health.

324 Finally, literature reports very efficient gas barrier coatings, constituted by ethylene vinyl alcohol
325 (EVOH) and PVOH; for example, 99.9 % reduction of OTR was achieved with EVOH coatings on PE
326 films (Krepker et al., 2018) and 99.2 % and 93.2 % of OTR reductions were achieved with EVOH and
327 PVOH coatings, respectively, on PET (Rovera et al., 2020). However, in the case of these polymer
328 coatings it is to be taken into account that they are usually of micrometric thickness and they can
329 significantly affect the recyclability of the final material.

330 The coating stability of the realized films in water was evaluated in order to evaluate the feasibility
331 of further painting the coated side of the films with aqueous lacquers. Stability tests were performed

332 by immersing the coated films in distilled water up to 24 h, according to the procedure detailed in
 333 the experimental section. The amount of graphene oxide released from the coating by water
 334 immersion for 24h at room temperature was evaluated and results are summarized in Table 2. As
 335 shown, the stability of the coating in water is very high, since for all the developed systems the
 336 amount of GO released from the coatings after 24 h of immersion is almost negligible, i.e. 1% or less
 337 for GO coatings and less than 1.5% for GO-MMT coatings. The higher amount of GO released from
 338 the hybrids can be explained by the lower interactions established by the GO and the phyllosilicate
 339 with respect to those established amongst GO sheets.

340 Water contact angle measurements (Figure S3) showed a high hydrophilic behaviour of the coated
 341 surfaces in comparison to pristine PE and PP surfaces. As shown in Table 2, CA decreased from 91°
 342 and 80° for the pristine PE and PP films to values ranging between 71° and 77°, slightly lower in the
 343 case of GO or GO-MMT coatings applied onto the PP substrate. Lower values of CA for PP systems,
 344 including the pristine PP film, are ascribable to the presence of slipping agents, such as fatty amides,
 345 usually employed in the production of polypropylene films (Hahladakis et al., 2018).

346

347 Table 2. Amount of released graphene from coated flexible films by water immersion and water contact
 348 angle of coated films
 349

Sample	Released GO (mg/m ²)	Amount of released GO with respect to the amount of GO in the coating (%)	Water contact angle (degrees)
PE	-	-	91
PE-GO	2.01	0.72	77
PE-GO-MMT	1.49	1.07	76
PP	-	-	80
PP-GO	2.85	1.01	74
PP-GO-MMT	2.04	1.45	71

350

351 Thus, the combined analysis of the stability tests and the water contact angle measurements
 352 indicated that the applied coatings are resistant to water despite being more affine to aqueous
 353 media than the pristine films. This demonstrate that the coatings are suitable for further surface
 354 treatments with water-based products, such as external inks and lacquers usually applied at
 355 industrial scale on flexible packaging films.

356

357

358

359 **3.2 Recycling tests**

360 As detailed in the experimental section and schematized in Figure 1, the PE and PP films with the
 361 GO and the hybrid GO-MMT coatings were subjected to reprocessing tests to evaluate their
 362 recyclability. The processing temperatures were selected taking into consideration the torque
 363 visualized during the extrusion process and the melting temperatures of the PE and PP films
 364 measured by DSC (120 °C and 160 °C for PE and PP, respectively). More in detail, the extrusion
 365 temperatures were set to maximize the viscosity of the polymer melt, in order to promote the
 366 effective dispersion of the nanostructured phase (deriving from the coating fragmentation) in the
 367 polymer melt. For PE the extrusion temperature was set 15°C above the melting temperature due
 368 to its very low MFR (0.644 g/10min) while for PP the quite high MFR (4.573 g/10min) allowed to set
 369 the extrusion temperature very close to its melting point. After a lab scale compounding test (see
 370 Figure 1b), nanocomposite pellets were obtained and further processed by compression moulding
 371 to realize recycled films (Figure 1c). No virgin PE or PP was added during the reprocessing. Therefore,
 372 the compositions of the recycled films, embedding the GO and the GO-MMT phases, correspond to
 373 the composition of the coated products. Codes and composition of the recycled materials are
 374 summarized in Table 3.

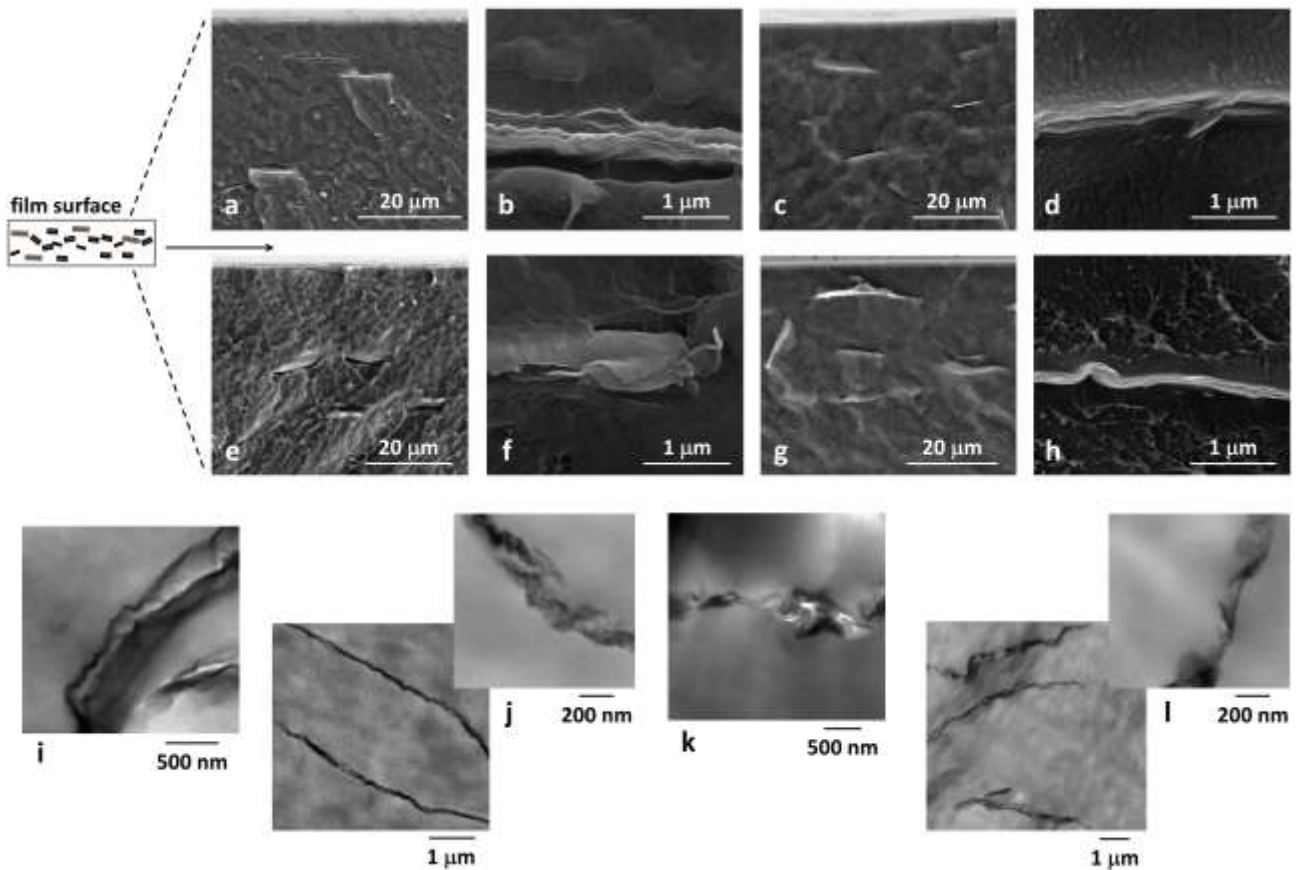
375

376 Table 3. Codes, compositions* and tensile properties (Young's modulus (E), stress at yield (σ_s) and
 377 elongation at break (ϵ_B)) of recycled PE and PP based samples
 378

Sample	PE or PP content (wt%)	GO (wt%)	MMT (wt%)	E (MPa)	σ_s (MPa)	ϵ_B (%)
PE_R	100	-	-	114 ± 3	7.8 ± 0.4	662 ± 73
PE-GO_R	99.58	0.42	-	100 ± 5	7.3 ± 0.2	921 ± 78
PE-GO-MMT_R	99.58	0.21	0.21	113 ± 10	7.6 ± 0.1	795 ± 165
PP_R	100	-	-	750 ± 88	20.7 ± 3.1	71 ± 7
PP-GO_R	99.40	0.60	-	638 ± 28	20.2 ± 4.6	26 ± 17
PP-GO-MMT_R	99.40	0.30	0.30	740 ± 33	24.4 ± 2.8	32 ± 21

379 * Different compositions amongst recycled PE and PP based systems depend on the different thickness of
 380 the pristine films.
 381

382 As evidenced from the Figure 1, all the samples showed a pronounced dark coloration due to the
 383 dispersion of the GO and GO-MMT phases in the polymer matrix promoted by the extrusion
 384 reprocessing. The morphology and structure of the obtained films was evaluated by SEM and TEM.
 385 Results are shown in Figure 3.
 386



387
 388 Figure 3. SEM images of the cryo-fractured cross sections of PE-GO_R (a, b), PP-GO_R (c, d), PE-GO-MMT_R
 389 (e, f) and PP-GO-MMT_R (g, h). The horizontal sides of SEM images are oriented along the film surfaces.

390 Bright field TEM images of PE-GO_R (i), PP-GO_R (j), PE-GO-MMT_R (k) and PP-GO-MMT_R (l)

391
 392 SEM images at low magnification (Figure 3a,c,e,g) revealed the cross-sectional structure of the
 393 recycled samples. After extrusion and compression moulding, 2D nanostructures with an
 394 approximate lateral size ranging between 10 and 35 μm were evidenced. These platelet-like
 395 nanostructures are oriented along the direction parallel to the surfaces of the film and their
 396 approximate thickness is slightly higher ($< 1 \mu\text{m}$) for PE-GO_R and PE-GO-MMT_R, whereas they are
 397 more compact, with thickness close to 200 nm, for PP-GO_R and PP-GO-MMT_R. The features of
 398 these platelet-like nanostructures are confirmed by TEM analysis (Figures 3i-l), that showed a more
 399 compact structure for the platelets embedded in PP-based recycled samples.

400 It seems evident that the platelet-like structures derive from the original GO and hybrid GO-MMT
 401 coatings applied on the PE and PP substrates, that during reprocessing are broken down in large
 402 platelets with lateral thickness $< 40 \mu\text{m}$ and dispersed in the polymer matrices. For PE-based
 403 samples, TEM images show that, after reprocessing, the GO and GO-MMT platelets appear partially
 404 exfoliated with respect to their pristine stacked form. Indeed, the GO and GO-MMT phases

405 dispersed in the PE polymer matrix are thicker than the pristine coating, up to 350 – 400 nm, possibly
406 because the PE phase has partially intermingled within the pristine coating structure. On the
407 contrary, when the PP-based samples were recycled, the compact structure of the coatings resulted
408 almost unaffected, with the thickness of the dispersed platelets comparable to the nominal
409 thickness (140 – 200 nm) of the original coatings. This phenomenon could be explained on the basis
410 of the very different melt behaviour of PE and PP, as revealed by their previously reported different
411 MFR. PE is significantly more viscous than PP in the tested conditions, and these differences are
412 certainly emphasized by the extrusion conditions employed for the recycling of the films. Therefore,
413 while the extrusion of PE is characterized by higher shear stresses that enable the partial exfoliation
414 of the nanostructured platelets, the extrusion of PP films is characterized by lower mixing stresses.
415 Despite the orientation of the lamellar nanostructures, the recycled films showed oxygen
416 permeability values comparable to those recorded for the pristine films (see Table S1), irrespectively
417 of the presence of the nanofillers. This can be ascribed to the very low content of nanostructured
418 materials contained in the recycled films, lower than 0.4 vol %, that is not enough to create an
419 effective tortuous path able to induce a permeability reduction to oxygen and water vapour in
420 comparison to high gas barrier properties nanocomposites, usually containing 1-3 vol % of lamellar
421 nanofillers (Wolf et al., 2018).

422 Finally, the recycled films were mechanically characterized by tensile tests. Results are shown in
423 Table 3. The mechanical properties recorded for the pristine PE and PP films are reported for
424 comparison in Table S2. To be noticed is that the thin GO and GO-MMT coating have negligible
425 effects on tensile properties of the films.

426 As shown, in the case of PE based systems, the recycling only induced a slight decrease of the
427 modulus and the stress at yield with respect to the pristine PE film, while the elongation was
428 retained or even increased. The recycling of the coated samples resulted in materials (PE-GO_R and
429 PE-GO-MMT_R) whose mechanical properties are essentially unchanged with respect to PE_R,
430 confirming that the low amount of nanostructured coating, partially exfoliated during the
431 reprocessing as shown by SEM/TEM analyses, does not affect the properties of the recycled
432 materials.

433 For PP based materials, a strong effect of the recycling process is observed already for the uncoated
434 sample: PP_R shows in fact a higher stiffness and much lower ultimate elongation with respect to
435 pristine PP film. This finding can be explained considering that the industrial production of cast
436 polypropylene results in an optimized film structure (in terms of crystallinity and macromolecular

437 arrangement) than cannot be reproduced through the lab scale compression moulding process
438 (Lamberti et al., 2002; Sacco et al., 2020). Indeed, as shown in Figure S4, the intensity ratio between
439 the FTIR absorption peaks centred at 841 cm^{-1} , typical of the crystalline phase, and at 973 cm^{-1} ,
440 typical of the amorphous phase (Lamberti et al., 2002), is much more intense for the recycled PP_R
441 sample ($I_{841}/I_{973} = 0.87$) with respect to the pristine PP film ($I_{841}/I_{973} = 0.74$). Also, the crystallinity
442 degree of PP and PP_R were evaluated by DSC analysis, which confirmed an increase of crystallinity
443 from 34.6 % (PP) to 40.5 % (PP_R) upon recycling. This makes the mechanical response of PP_R non
444 directly comparable to that shown by neat PP films. Thus, limiting the discussion to the recycled
445 samples, also for the recycled polypropylene samples the presence of the filler showed negligible
446 effects on the polymer stiffness and strength, and only slightly reduced the maximum elongation of
447 the system, as often found in PP based nanocomposite systems, in which the filler usually acts as a
448 defect point that promote an early rupture of the specimen during the tensile deformation in
449 comparison to the unfilled matrix (Dittrich et al., 2013). Furthermore, in Figure S4 signals at 1645 cm^{-1} ,
450 3190 cm^{-1} and 3390 cm^{-1} associated to carbonyl stretching and to the stretching vibrations of
451 the NH_2 group may be indicative of the presence of fatty amides usually used in polyolefins as anti-
452 static and slip agents, such as erucamide (Dulal et al., 2018; Gall et al., 2020).

453 Water stability tests were also performed on the recycled nanocomposite films, which showed no
454 detectable graphene oxide release upon water immersion for 24h at room temperature. Indeed, in
455 this case, the nanoparticles are well embedded in the polymer matrix of the nanocomposite films,
456 as evidenced by SEM and TEM analyses, and therefore cannot be released to water.

457 Therefore, all results well demonstrate that by applying a design-for-recycling approach and
458 exploiting the knowledge on advanced and nanostructured materials it is possible to develop novel
459 high-performance flexible films that could replace current non-recyclable products. Despite the
460 proposed solution is specific for a particular class of products, namely flexible packaging film, the
461 proposed methodology has a general character and can be extended to different products of the
462 food packaging sector.

463 These objectives well match the Sustainable Development Goals (SDGs) defined in the 2030 Agenda
464 for Sustainable Development, adopted by all United Nations Member States in December 2017, that
465 set the target of 55% recycling of plastic packaging waste by 2030 by banning landfilling and
466 adopting stricter agreements on extended producer responsibility (EPR). By 2030, all plastic
467 packaging will need to be designed to be recyclable or reusable to contribute effectively to food

468 security, sustainable industry, sustainable cities and communities, responsible consumption and
469 production.

470

471 **5. Conclusions**

472 New recyclable-by-design mono-material flexible films with high barrier properties to gases and UV
473 radiation have been developed by applying graphene oxide and graphene oxide/montmorillonite
474 hybrid coatings on low density polyethylene and polypropylene substrates.

475 The coatings have induced remarkable UV barrier, quantified as a transmittance reduction at 400
476 nm wavelength of 40-60%. Moreover, by the application of the coatings, oxygen permeability has
477 been reduced of 97.5-98.5% for polyethylene and of 94.0-96.5% for polypropylene. The water
478 vapour transmission rate was reduced of 68.0-72.5% for polyethylene and of 70.4-78.8% for
479 polypropylene.

480 To demonstrate their recyclability, reprocessing tests by lab scale extrusion have been performed
481 on the coated films. After extrusion and compression moulding, homogeneously distributed 2D
482 nanostructures deriving from the fragmentation of the original coatings and the dispersion of the
483 obtained stacked platelets in the polymer matrices have been evidenced in the cross-section of the
484 recycled samples. These platelets have been found well oriented along the film direction. In the case
485 of polyethylene films, an intermingling of the polymer phase within the platelets has been also
486 evidenced. What is to be remarked is that the presence of the nanofillers in the recycled samples
487 has not significantly affected the mechanical properties of the polymers with respect to the recycled
488 pristine films.

489 Both the coated films and the recycled films are stable, with low release of GO from the coatings
490 and no appreciable release of GO from the recycled samples by water immersion for 24h at room
491 temperature.

492 A scale-up phase of the proposed process will be needed to optimize the coating application and
493 further validate at industrial scale the achieved outcomes. Nevertheless, the results obtained in this
494 work confirm that the application of graphene based coatings to realize mono-material gas barrier
495 films for packaging applications is a promising effective strategy to realize high performance
496 products able to be easily recycled, thus showing a new sustainable end-of-life option with respect
497 to current products.

498

499 **Acknowledgments**

500 This work has been co-financed by the Italian Ministry of Economic Development (MISE) as part of
501 the R&D project “Film for food packaging with improved barrier properties and recyclability by
502 coatings and adhesives based on 2D nanostructured fillers” Call Horizon 2020 – PON 2014-2020, DM
503 01/06/2016, CUP: B78I17000160008.

504

505 References

- 506 Ahamed, A., Veksha, A., Giannis, A., & Lisak, G. (2021). Flexible packaging plastic waste –
507 environmental implications, management solutions, and the way forward. In *Current Opinion*
508 *in Chemical Engineering* (Vol. 32, p. 100684). Elsevier.
509 <https://doi.org/10.1016/j.coche.2021.100684>
- 510 Anukiruthika, T., Sethupathy, P., Wilson, A., Kashampur, K., Moses, J. A., & Anandharamakrishnan,
511 C. (2020). Multilayer packaging: Advances in preparation techniques and emerging food
512 applications. *Comprehensive Reviews in Food Science and Food Safety*, 19(3), 1156–1186.
513 <https://doi.org/10.1111/1541-4337.12556>
- 514 Asmatulu, R., Khan, W. S., Reddy, R. J., & Ceylan, M. (2015). Synthesis and analysis of injection-
515 molded nanocomposites of recycled high-density polyethylene incorporated with graphene
516 nanoflakes. *Polymer Composites*, 36(9), 1565–1573. <https://doi.org/10.1002/pc.23063>
- 517 Avella, M., Bruno, G., Errico, M. E., Gentile, G., Piciocchi, N., Sorrentino, A., & Volpe, M. G. (2007).
518 Innovative packaging for minimally processed fruits. *Packaging Technology and Science*,
519 20(5), 325–335. <https://doi.org/10.1002/pts.761>
- 520 Avella, Maurizio, Avolio, R., Bonadies, I., Carfagna, C., Errico, M. E., & Gentile, G. (2009). Recycled
521 multilayer cartons as cellulose source in HDPE-based composites: Compatibilization and
522 structure-properties relationships. *Journal of Applied Polymer Science*, 114(5), 2978–2985.
523 <https://doi.org/10.1002/app.30913>
- 524 Avolio, R., Gentile, G., Avella, M., Carfagna, C., & Errico, M. E. (2013). Polymer–filler interactions in
525 PET/CaCO₃ nanocomposites: Chain ordering at the interface and physical properties.
526 *European Polymer Journal*, 49(2), 419–427.
527 <https://doi.org/10.1016/J.EURPOLYMJ.2012.10.008>
- 528 Barlow, C. Y., & Morgan, D. C. (2013). Polymer film packaging for food: An environmental
529 assessment. In *Resources, Conservation and Recycling* (Vol. 78, pp. 74–80). Elsevier.
530 <https://doi.org/10.1016/j.resconrec.2013.07.003>
- 531 Botta, L., Scaffaro, R., Suter, F., & Mistretta, M. C. (2018). Reprocessing of PLA/graphene
532 nanoplatelets nanocomposites. *Polymers*, 10(1), 18. <https://doi.org/10.3390/polym10010018>
- 533 Castaldo, R., Lama, G. C., Aprea, P., Gentile, G., Ambrogio, V., Lavorgna, M., & Cerruti, P. (2019).
534 Humidity-Driven Mechanical and Electrical Response of Graphene/Cloisite Hybrid Films.
535 *Advanced Functional Materials*, 29(14). <https://doi.org/10.1002/adfm.201807744>
- 536 Castaldo, R., Lama, G. C., Aprea, P., Gentile, G., Lavorgna, M., Ambrogio, V., & Cerruti, P. (2018).
537 Effect of the oxidation degree on self-assembly, adsorption and barrier properties of nano-
538 graphene. *Microporous and Mesoporous Materials*, 260(August 2017), 102–115.
539 <https://doi.org/10.1016/j.micromeso.2017.10.026>
- 540 Ceflex, 2020. Designing for a Circular Economy. <https://guidelines.ceflex.eu/> (accessed 21
541 September 2021)
- 542 Chen, G. G., Qi, X. M., Li, M. P., Guan, Y., Bian, J., Peng, F., Yao, C. L., & Sun, R. C. (2015).
543 Hemicelluloses/montmorillonite hybrid films with improved mechanical and barrier
544 properties. *Scientific Reports*, 5(1), 1–12. <https://doi.org/10.1038/srep16405>

545 Chen, R. S., Ahmad, S., & Gan, S. (2017). Characterization of recycled thermoplastics-based
546 nanocomposites: Polymer-clay compatibility, blending procedure, processing condition, and
547 clay content effects. *Composites Part B: Engineering*, *131*, 91–99.
548 <https://doi.org/10.1016/j.compositesb.2017.07.057>

549 Chowreddy, R. R., Nord-Varhaug, K., & Rapp, F. (2019). Recycled Poly(Ethylene
550 Terephthalate)/Clay Nanocomposites: Rheology, Thermal and Mechanical Properties. *Journal
551 of Polymers and the Environment*, *27*(1), 37–49. <https://doi.org/10.1007/s10924-018-1320-6>

552 Despoudi, S. (2020). Circular food supply chains. *Food Science and Technology*, *34*(1), 48–51.
553 https://doi.org/10.1002/fsat.3401_13.x

554 Dittrich, B., Wartig, K.-A., Hofmann, D., Mülhaupt, R., & Schartel, B. (2013). Carbon black, multiwall
555 carbon nanotubes, expanded graphite and functionalized graphene flame retarded
556 polypropylene nanocomposites. *Polymers for Advanced Technologies*, *24*(10), 916–926.
557 <https://doi.org/10.1002/PAT.3165>

558 Ellis, T. S., & D'Angelo, J. S. (2003). Thermal and mechanical properties of a polypropylene
559 nanocomposite. *Journal of Applied Polymer Science*, *90*(6), 1639–1647.
560 <https://doi.org/10.1002/app.12830>

561 Eriksen, M. K., Christiansen, J. D., Daugaard, A. E., & Astrup, T. F. (2019). Closing the loop for PET,
562 PE and PP waste from households: Influence of material properties and product design for
563 plastic recycling. *Waste Management*, *96*, 75–85.
564 <https://doi.org/10.1016/j.wasman.2019.07.005>

565 European Commission, 2018. Questions & Answers: A European strategy for plastics.
566 https://ec.europa.eu/commission/presscorner/detail/sv/MEMO_18_6 (accessed 21
567 September 2021).

568 Findenig, G., Leimgruber, S., Kargl, R., Spirk, S., Stana-Kleinschek, K., & Ribitsch, V. (2012). Creating
569 water vapor barrier coatings from hydrophilic components. *ACS Applied Materials and
570 Interfaces*, *4*(6), 3199–3206. <https://doi.org/10.1021/am300542h>

571 Goudarzi, V., Shahabi-Ghahfarrokhi, I., & Babaei-Ghazvini, A. (2017). Preparation of ecofriendly
572 UV-protective food packaging material by starch/TiO₂ bio-nanocomposite: Characterization.
573 *International Journal of Biological Macromolecules*, *95*, 306–313.
574 <https://doi.org/10.1016/j.ijbiomac.2016.11.065>

575 Grace, R. (2019). New Mono-Material Flexible Pouch Follows Cradle to Cradle Principles: Werner &
576 Mertz partners with Mondi, three others to close the loop on package design. *Plastics
577 Engineering*, *75*(1), 14–19. <https://doi.org/10.1002/peng.20053>

578 Guillard, V., Gaucel, S., Fornaciari, C., Angellier-Coussy, H., Buche, P., & Gontard, N. (2018). The
579 Next Generation of Sustainable Food Packaging to Preserve Our Environment in a Circular
580 Economy Context. *Frontiers in Nutrition*, *5*(December), 1–13.
581 <https://doi.org/10.3389/fnut.2018.00121>

582 Gusev, A. A., & Lusti, H. R. (2001). Rational design of nanocomposites for barrier applications.
583 *Advanced Materials*, *13*(21), 1641–1643. [https://doi.org/10.1002/1521-4095\(200111\)13:21<1641::AID-ADMA1641>3.0.CO;2-P](https://doi.org/10.1002/1521-4095(200111)13:21<1641::AID-ADMA1641>3.0.CO;2-P)

584 Hahladakis, J. N., Velis, C. A., Weber, R., Iacovidou, E., & Purnell, P. (2018). An overview of
585 chemical additives present in plastics: Migration, release, fate and environmental impact
586 during their use, disposal and recycling. *Journal of Hazardous Materials*, *344*, 179–199.
587 <https://doi.org/10.1016/J.JHAZMAT.2017.10.014>

588 Heo, J., Choi, M., & Hong, J. (2019). Facile Surface Modification of Polyethylene Film via Spray-
589 Assisted Layer-by-Layer Self-Assembly of Graphene Oxide for Oxygen Barrier Properties.
590 *Scientific Reports*, *9*(1), 1–7. <https://doi.org/10.1038/s41598-019-39285-0>

591 Hirvikorpi, T., Vähä-Nissi, M., Mustonen, T., Iiskola, E., & Karppinen, M. (2010). Atomic layer
592

593 deposited aluminum oxide barrier coatings for packaging materials. *Thin Solid Films*, 518(10),
594 2654–2658. <https://doi.org/10.1016/J.TSF.2009.08.025>

595 Horodytska, O., Valdés, F. J., & Fullana, A. (2018). Plastic flexible films waste management – A
596 state of art review. In *Waste Management* (Vol. 77, pp. 413–425). Waste Manag.
597 <https://doi.org/10.1016/j.wasman.2018.04.023>

598 Istrate, O. M., & Chen, B. (2018). Structure and properties of clay/recycled plastic composites.
599 *Applied Clay Science*, 156, 144–151. <https://doi.org/10.1016/j.clay.2018.01.039>

600 Kaiser, K., Schmid, M., & Schlummer, M. (2018). Recycling of polymer-based multilayer packaging:
601 A review. In *Recycling* (Vol. 3, Issue 1, p. 1). Multidisciplinary Digital Publishing Institute.
602 <https://doi.org/10.3390/recycling3010001>

603 Kirchheim, D., Jaritz, M., Wilski, S., Hopmann, C., & Dahlmann, R. (n.d.). *Transport mechanisms of*
604 *water vapour and oxygen through SiO_x coated polypropylene*.

605 Krepker, M., Zhang, C., Nitzan, N., Prinz-Setter, O., Massad-Ivanir, N., Olah, A., Baer, E., & Segal, E.
606 (2018). Antimicrobial LDPE/EVOH Layered Films Containing Carvacrol Fabricated by
607 Multiplication Extrusion. *Polymers* 2018, Vol. 10, Page 864, 10(8), 864.
608 <https://doi.org/10.3390/POLYM10080864>

609 Lamberti, G., Brucato, V., & Titomanlio, G. (2002). Orientation and crystallinity in film casting of
610 polypropylene. *Journal of Applied Polymer Science*, 84(11), 1981–1992.
611 <https://doi.org/10.1002/app.10422>

612 Laridon, Y., Touchaleaume, F., Gontard, N., & Peyron, S. (2020). Food-grade PE recycling: Effect of
613 nanoclays on the decontamination efficacy. *Polymers*, 12(4), 822.
614 <https://doi.org/10.3390/POLYM12040822>

615 Li, H., Yang, L., Wang, Z., Liu, Z., & Chen, Q. (n.d.). *molecules Pre-grafted Group on PE Surface by*
616 *DBD Plasma and Its Influence on the Oxygen Permeation with Coated SiO_x*.
617 <https://doi.org/10.3390/molecules24040780>

618 Lim, J. W., Lim, W. S., Lee, M. H., & Park, H. J. (2021). Barrier and structural properties of
619 polyethylene terephthalate film coated with poly(acrylic acid)/montmorillonite
620 nanocomposites. *Packaging Technology and Science*, 34(3), 141–150.
621 <https://doi.org/10.1002/pts.2547>

622 Liu, F., Dai, R., Zhu, J., & Li, X. (2010). Optimizing color and lipid stability of beef patties with a
623 mixture design incorporating with tea catechins, carnosine, and α-tocopherol. *Journal of Food*
624 *Engineering*, 98(2), 170–177. <https://doi.org/10.1016/J.JFOODENG.2009.12.023>

625 López de Dicastillo, C., Velásquez, E., Rojas, A., Guarda, A., & Galotto, M. J. (2020). The use of
626 nanoadditives within recycled polymers for food packaging: Properties, recyclability, and
627 safety. *Comprehensive Reviews in Food Science and Food Safety*, 19(4), 1760–1776.
628 <https://doi.org/10.1111/1541-4337.12575>

629 Ma, Y. (2018). Changing Tetra Pak: From Waste to Resource: *Science Progress*, 101(2), 161–170.
630 <https://doi.org/10.3184/003685018X15215434299329>

631 Marsh, K., & Bugusu, B. (2007). Food Packaging—Roles, Materials, and Environmental Issues.
632 *Journal of Food Science*, 72(3), R39–R55. <https://doi.org/10.1111/J.1750-3841.2007.00301.X>

633 Mourad, A. L., Garcia, E. E. C., Vilela, G. B., & Von Zuben, F. (2008). Influence of recycling rate
634 increase of aseptic carton for long-life milk on GWP reduction. *Resources, Conservation and*
635 *Recycling*, 52(4), 678–689. <https://doi.org/10.1016/j.resconrec.2007.09.001>

636 Okada, A., & Usuki, A. (2006). Twenty Years of Polymer-Clay Nanocomposites. *Macromolecular*
637 *Materials and Engineering*, 291(12), 1449–1476. <https://doi.org/10.1002/MAME.200600260>

638 Pang, A. L., Husin, M. R., Arsad, A., & Ahmadipour, M. (2021). Effect of graphene nanoplatelets on
639 structural, morphological, thermal, and electrical properties of recycled
640 polypropylene/polyaniline nanocomposites. *Journal of Materials Science: Materials in*

641 *Electronics*, 32(7), 9574–9583. <https://doi.org/10.1007/s10854-021-05620-3>

642 Pettersen, M. K., Grøvlen, M. S., Evje, N., & Radusin, T. (2020). Recyclable mono materials for
643 packaging of fresh chicken fillets: New design for recycling in circular economy. *Packaging*
644 *Technology and Science*, 33(11), 485–498. <https://doi.org/10.1002/pts.2527>

645 Pierleoni, D., Xia, Z. Y., Christian, M., Ligi, S., Minelli, M., Morandi, V., Doghieri, F., & Palermo, V.
646 (2016). Graphene-based coatings on polymer films for gas barrier applications. *Carbon*, 96,
647 503–512. <https://doi.org/10.1016/j.carbon.2015.09.090>

648 PlasticsEurope, 2020. Plastics - the Facts 2020 report.
649 <https://www.plasticseurope.org/it/resources/publications/4312-plastics-facts-2020> (accessed
650 21 September 2021)

651 Plastics Recyclers Europe, 2021. Challenges and Opportunities.
652 <https://www.plasticsrecyclers.eu/challenges-and-opportunities> (accessed 21 September
653 2021)

654 Ragaert, K., Huysveld, S., Vyncke, G., Hubo, S., Veelaert, L., Dewulf, J., & Du Bois, E. (2020). Design
655 from recycling: A complex mixed plastic waste case study. *Resources, Conservation and*
656 *Recycling*, 155, 104646. <https://doi.org/10.1016/j.resconrec.2019.104646>

657 RecyClass, 2020. Recyclability Methodology. <https://recyclclass.eu/recyclclass/methodology/>
658 (accessed 21 September 2021)

659 Rigail-Cedeño, A., Diaz-Barrios, A., Gallardo-Bastidas, J., Ullaguari-Loor, S., & Morales-Fuentes, N.
660 (2019). Recycled HDPE/PET clay nanocomposites. *Key Engineering Materials*, 821 KEM, 67–
661 73. <https://doi.org/10.4028/WWW.SCIENTIFIC.NET/KEM.821.67>

662 Rovera, C., Ghaani, M., & Farris, S. (2020). Nano-inspired oxygen barrier coatings for food
663 packaging applications: An overview. In *Trends in Food Science and Technology* (Vol. 97, pp.
664 210–220). Elsevier Ltd. <https://doi.org/10.1016/j.tifs.2020.01.024>

665 Ruengkajorn, K., Chen, C., Yu, J., Buffet, J. C., & O'Hare, D. (2021). Non-toxic layered double
666 hydroxide nanoplatelet dispersions for gas barrier coatings on flexible packaging. *Materials*
667 *Advances*, 2(8), 2626–2635. <https://doi.org/10.1039/d0ma00986e>

668 Sacco, F. Di, Gahleitner, M., Wang, J., & Portale, G. (2020). Systematic Investigation on the
669 Structure-Property Relationship in Isotactic Polypropylene Films Processed via Cast Film
670 Extrusion. *Polymers 2020*, Vol. 12, Page 1636, 12(8), 1636.
671 <https://doi.org/10.3390/POLYM12081636>

672 Scherillo, G., Lavorgna, M., Buonocore, G. G., Zhan, Y. H., Xia, H. S., Mensitieri, G., & Ambrosio, L.
673 (2014). Tailoring assembly of reduced graphene oxide nanosheets to control gas barrier
674 properties of natural rubber nanocomposites. *ACS Applied Materials and Interfaces*, 6(4),
675 2230–2234. <https://doi.org/10.1021/am405768m>

676 Srebrenkoska, V., Gaceva, G. B., Avella, M., Ericco, M. E., & Gentile, G. (2009). Utilization of
677 Recycled Polypropylene for Production of Eco-Composites.
678 [Http://Dx.Doi.Org/10.1080/03602550903147247](http://Dx.Doi.Org/10.1080/03602550903147247), 48(11), 1113–1120.
679 <https://doi.org/10.1080/03602550903147247>

680 Struller, C. F., Kelly, P. J., & Copeland, N. J. (2014). Aluminum oxide barrier coatings on polymer
681 films for food packaging applications. *Surface and Coatings Technology*, 241, 130–137.
682 <https://doi.org/10.1016/J.SURFCOAT.2013.08.011>

683 Triantou, M., Todorova, N., Giannakopoulou, T., Vaimakis, T., & Trapalis, C. (2017). Mechanical
684 performance of re-extruded and aged graphene/polypropylene nanocomposites. *Polymer*
685 *International*, 66(12), 1716–1724. <https://doi.org/10.1002/pi.5353>

686 Walker, T. W., Frelka, N., Shen, Z., Chew, A. K., Banick, J., Grey, S., Kim, M. S., Dumesic, J. A., Van
687 Lehn, R. C., & Huber, G. W. (2020). Recycling of multilayer plastic packaging materials by
688 solvent-targeted recovery and precipitation. *Science Advances*, 6(47).

689 <https://doi.org/10.1126/sciadv.aba7599>
690 Wolf, C., Angellier-Coussy, H., Gontard, N., Doghieri, F., & Guillard, V. (2018). How the shape of
691 fillers affects the barrier properties of polymer/non-porous particles nanocomposites: A
692 review. *Journal of Membrane Science*, 556(January), 393–418.
693 <https://doi.org/10.1016/j.memsci.2018.03.085>
694 Won, S., Van Lam, D., Lee, J. Y., Jung, H. J., Hur, M., Kim, K. S., Lee, H. J., & Kim, J. H. (2018).
695 Graphene-based stretchable and transparent moisture barrier. *Nanotechnology*, 29(12),
696 125705. <https://doi.org/10.1088/1361-6528/aaa8b1>
697 Yan, N., Capezzuto, F., Buonocore, G. G., Lavorgna, M., Xia, H., & Ambrosio, L. (2015). Gas-Barrier
698 Hybrid Coatings by the Assembly of Novel Poly(vinyl alcohol) and Reduced Graphene Oxide
699 Layers through Cross-Linking with Zirconium Adducts. *ACS Applied Materials and Interfaces*,
700 7(40), 22678–22685. <https://doi.org/10.1021/acsami.5b07529>
701 Yang, S., Bai, S., Duan, W., & Wang, Q. (2018). Production of Value-Added Composites from
702 Aluminum-Plastic Package Waste via Solid-State Shear Milling Process. *ACS Sustainable*
703 *Chemistry and Engineering*, 6(3), 4282–4293.
704 <https://doi.org/10.1021/acssuschemeng.7b04733>
705 Yoo, J., Lee, S. B., Lee, C. K., Hwang, S. W., Kim, C., Fujigaya, T., Nakashima, N., & Shim, J. K. (2014).
706 Graphene oxide and laponite composite films with high oxygen-barrier properties. *Nanoscale*,
707 6(18), 10824–10830. <https://doi.org/10.1039/c4nr03429e>
708 Yu, J., Ruengkajorn, K., Crivoi, D. G., Chen, C., Buffet, J. C., & O'Hare, D. (2019). High gas barrier
709 coating using non-toxic nanosheet dispersions for flexible food packaging film. *Nature*
710 *Communications*, 10(1), 1–8. <https://doi.org/10.1038/s41467-019-10362-2>
711 Yu, Y., Zheng, J., Li, J., Lu, L., Yan, J., Zhang, L., & Wang, L. (2021). Applications of two-dimensional
712 materials in food packaging. In *Trends in Food Science and Technology* (Vol. 110, pp. 443–
713 457). Elsevier. <https://doi.org/10.1016/j.tifs.2021.02.021>
714 Zare, Y. (2013). Recent progress on preparation and properties of nanocomposites from recycled
715 polymers: A review. *Waste Management*, 33(3), 598–604.
716 <https://doi.org/10.1016/j.wasman.2012.07.031>
717 Zdiri, K., Elamri, A., Hamdaoui, M., Harzallah, O., Khenoussi, N., & Brendlé, J. (2018).
718 Reinforcement of recycled pp polymers by nanoparticles incorporation. *Green Chemistry*
719 *Letters and Reviews*, 11(3), 296–311. <https://doi.org/10.1080/17518253.2018.1491645>
720 Zhan, Y., Meng, Y., Li, Y., Zhang, C., Xie, Q., Wei, S., Lavorgna, M., & Chen, Z. (2021). Poly(vinyl
721 alcohol)/reduced graphene oxide multilayered coatings: The effect of filler content on gas
722 barrier and surface resistivity properties. *Composites Communications*, 24, 100670.
723 <https://doi.org/10.1016/J.COCO.2021.100670>
724